

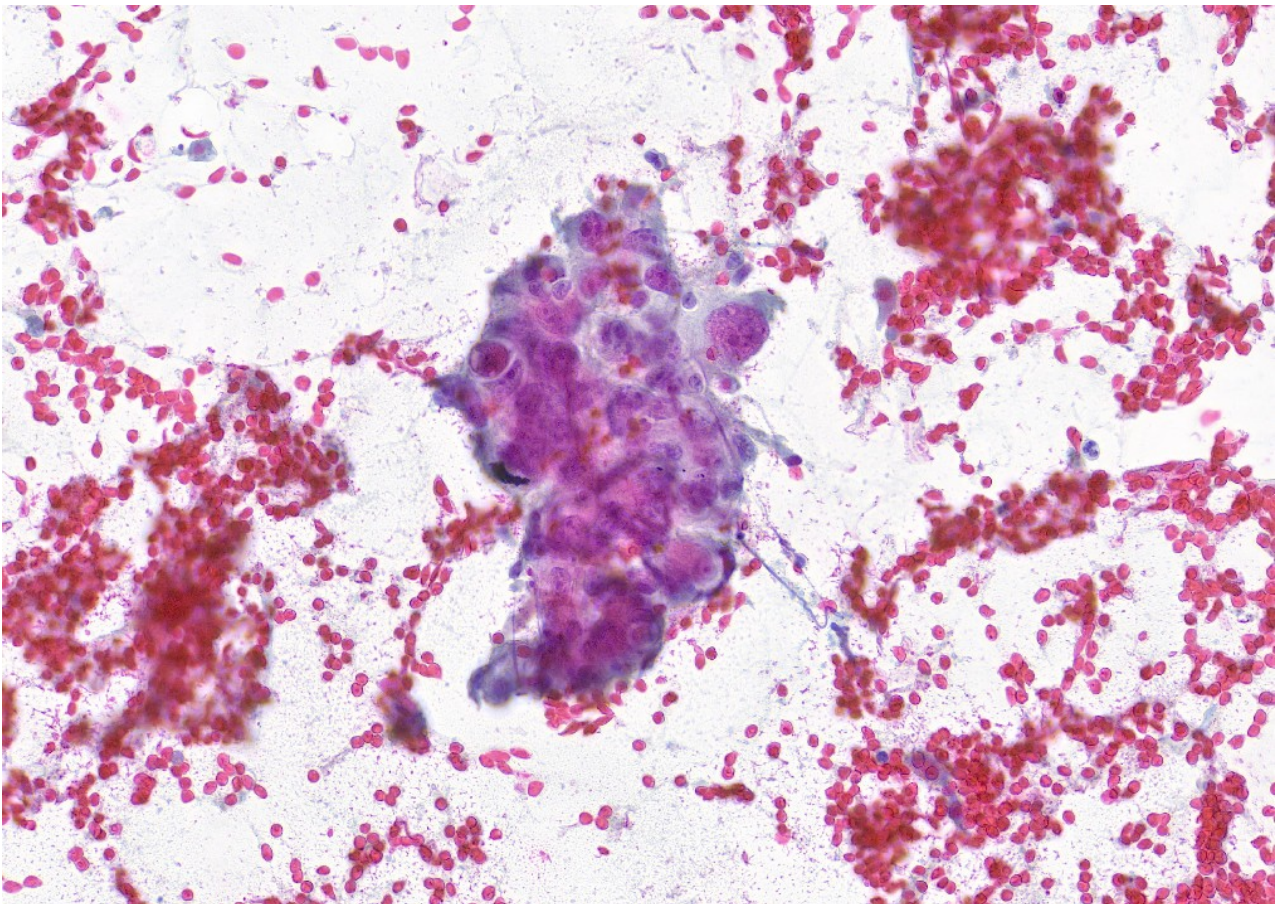
Anaplastic Thyroid Carcinoma with Suspected SMARCA4 Loss-of-Function

Mario Urso, School of Medicine and Surgery, Residency Program in Clinical Pathology and Clinical Biochemistry, University of Milano-Bicocca, Monza, Italy m.urso12@campus.unimib.it

Case Report

On 4 March, a 49-year-old man was referred to the Fine Needle Aspiration (FNA) Clinic at our hospital for evaluation of a large thyroid nodule. Neck ultrasound revealed a normally positioned thyroid gland with a 6 cm hypoechoic nodular mass at the isthmus. An ultrasound-guided FNA was performed in collaboration with the interventional radiology team. Two smears were prepared and immediately fixed for Papanicolaou staining.

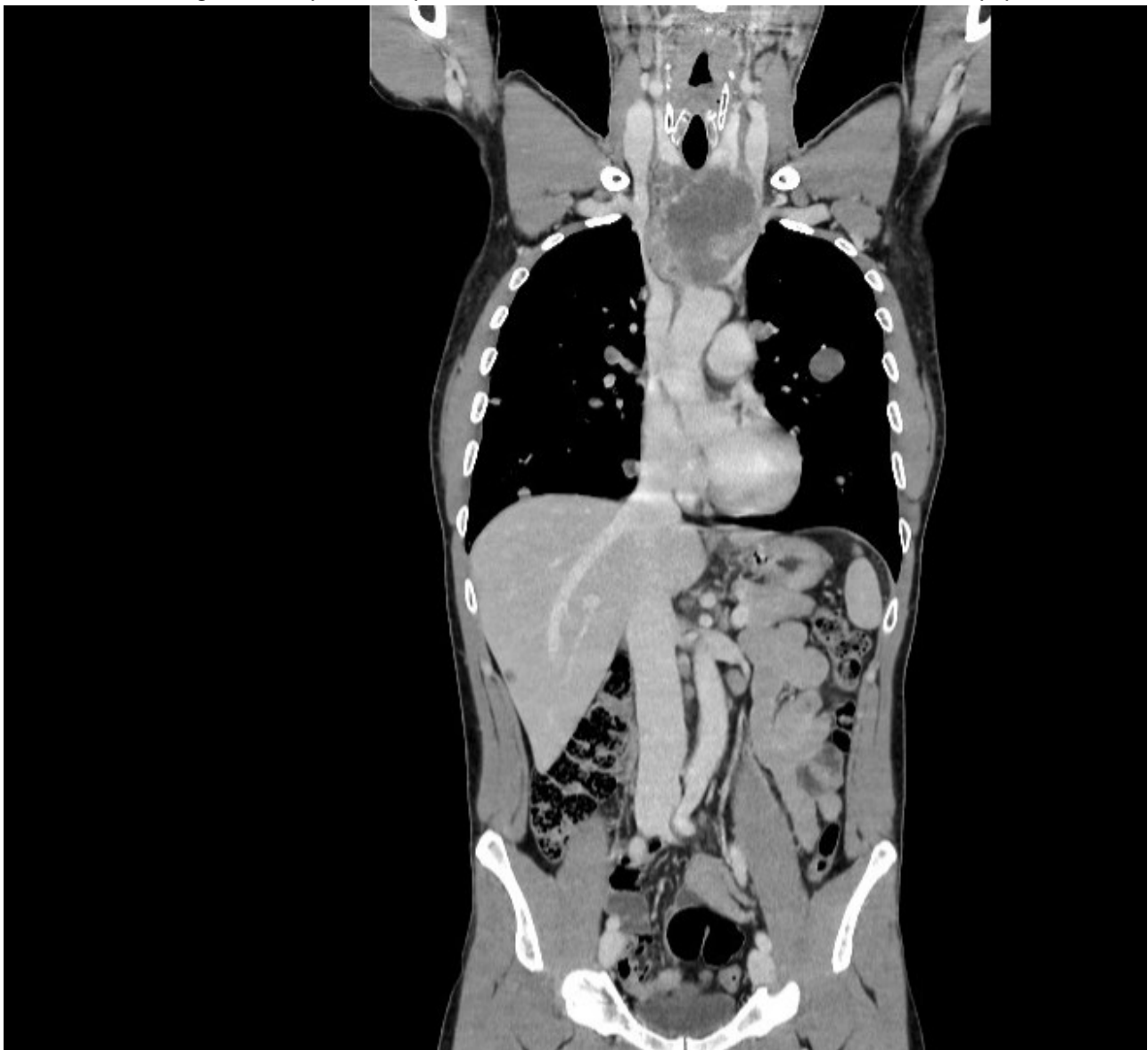
Cytological examination demonstrated pleomorphic cells with nuclear hyperchromasia, squamoid features, and apoptotic bodies in a necrotic background. These findings were consistent with anaplastic thyroid carcinoma (ATC) and were classified as TIR 5 according to the 2014 SIAPeC Italian Consensus (corresponding to malignant – Bethesda category VI, 2023) [Figure 1, 2 – Direct smear, Papanicolaou stain, 20x].



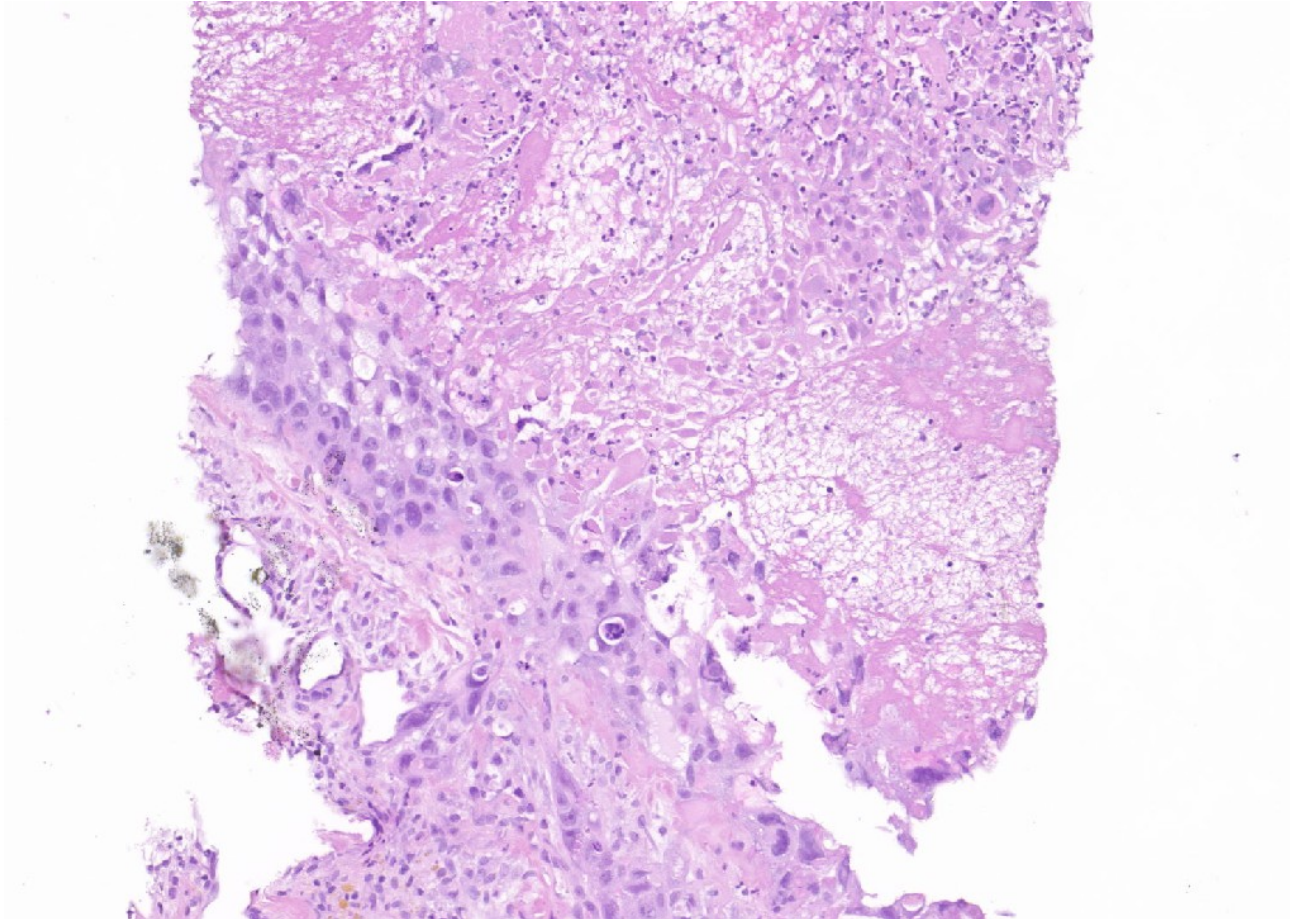
BRAF mutation analysis was requested. Prior to molecular testing, one Papanicolaou-stained cytological slide was digitised for medico-legal purposes. On the selected smear, tumour-rich areas showed ~80% cellularity. After manual scraping of the marked areas on the slide, DNA was extracted and purified using the Maxwell CSC 16 system (Promega) with the CSC DNA FFPE kit, and DNA quantity was assessed fluorometrically using Qubit 4.0 (Thermo Fisher Scientific). BRAF codon 600 mutations were tested via real-time PCR (EasyPGX® qPCR Instrument 96, Diatech Pharmacogenetics) using the EasyPGX® ready BRAF kit (CE-IVD), which detects V600E, V600Ecomplex, V600K, V600D, and V600R mutations with a sensitivity of 0.5–1%. No V600 mutations were identified.

Meanwhile, contrast-enhanced CT of the neck and chest revealed extensive local invasion, cervical and mediastinal lymphadenopathy, and multiple pulmonary nodules. Abdominal CT also showed splenic and intraaortocaval lesions [Figure 3 – Contrast enhanced neck, chest and abdomen CT].

Considering the extent of the disease, the impossibility of using additional cytology specimens, and the need to investigate other potentially actionable mutations, on 11 March a core needle biopsy (CNB) of the

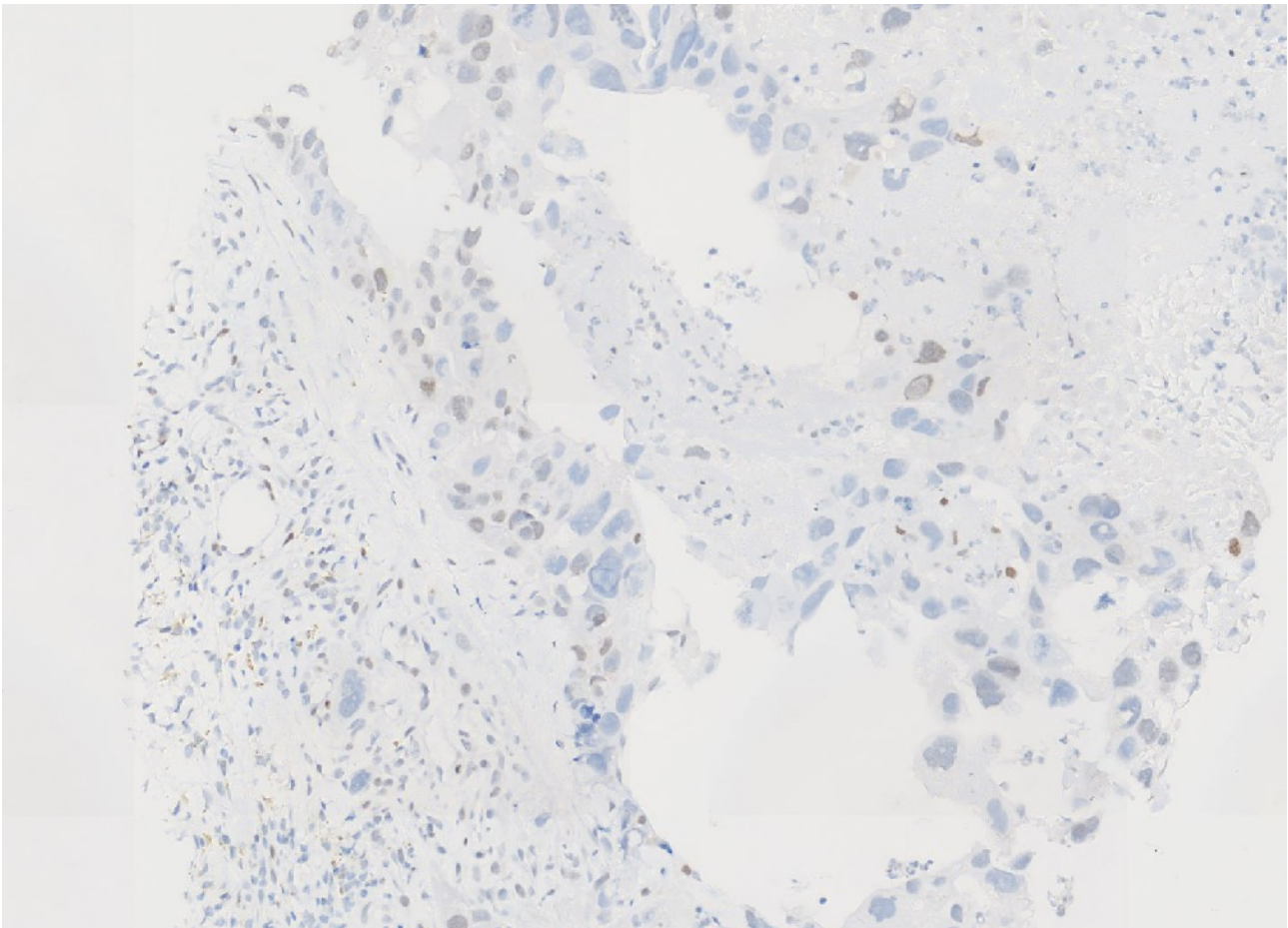


thyroid mass was performed to obtain sufficient tissue for NGS analysis and additional special stains (e.g., immunohistochemistry). The hematoxylin and eosin (H&E)-stained slide confirmed features previously observed in cytology, and revealed extensive areas of necrosis with an estimated neoplastic cellularity of ~25%. To overcome this limitation and ensure sufficient DNA yield for analysis, 10 unstained 8 µm sections were prepared for DNA extraction and quantification [Figure 4 –Core Needle Biopsy, H&E, 10x].



Sequencing was performed using the Genexus Integrated Sequencer (Thermo Fisher Scientific) with the OncoPrint Comprehensive Assay v3, covering 161 clinically relevant genes, including single nucleotide variants (SNVs), copy number alterations (CNAs), gene fusions, splice variants. Data analysis was conducted with Ion Torrent Genexus Software v6.8.1.1, using reference genome GRCh37/hg19 and nomenclature according to the Human Genome Variation Society. NGS analysis revealed a TP53 exon 5 nonsense mutation (c.489C>G; p.Y163, VAF 17%)* and a PTEN exon 5 frameshift mutation (c.475_478del; p.R159Pfs*7, VAF 13%). Therefore, no targetable mutations were detected.

Notably, a loss-of-function mutation in SMARCA4 was also identified. Given the potential diagnostic implications, immunohistochemical (IHC) staining for BRG1 (the SMARCA4 protein product) was performed on an additional biopsy section. IHC was carried out on the Ventana Benchmark ULTRA platform using an anti-BRG1 antibody (Abcam Cambridge, UK; 1:50) and showed heterogeneous BRG1 loss, suggesting a subclonal origin, rather than the diffuse expression loss expected in SMARCA4-deficient undifferentiated tumors of thoracic origin [Figure 5 – Core Needle Biopsy, anti-BRG1 stain, 10x]. Consequently, the initial diagnosis of ATC was confirmed. Despite treatment with immunotherapy, the patient experienced rapid disease progression and died on 26 March during hospitalisation in the medical oncology unit.



Discussion

Cytological smears of anaplastic thyroid carcinomas typically show pleomorphic epithelioid or spindle cells with nuclear enlargement, irregular membranes, necrosis, and an inflammatory background. However, low cellularity, extensive necrosis, and overlapping features with other high-grade malignancies can render the diagnosis of anaplastic thyroid carcinoma (ATC) particularly challenging, especially when further complicated by the absence of conventional thyroid markers such as TTF1 and PAX8, and the presence of atypical ones. In the present case, diagnostic uncertainty was heightened by the identification of a SMARCA4 loss-of-function mutation. This alteration is characteristic of a recently recognized subset of thoracic undifferentiated tumors, which may display purely sarcomatoid features or a combination of sarcomatous and carcinomatous components, typically associated with extensive necrosis, inflammation, and brisk mitotic activity. These overlapping morphological and molecular features initially raised suspicion for a metastatic SMARCA4-deficient undifferentiated thoracic tumor, particularly in light of radiological findings. However, subsequent immunohistochemical analysis excluded this diagnosis and supported the original interpretation.

Unfortunately, in this case, the patient did not have access to targeted therapies, as no clinically actionable mutations were identified. He experienced rapid disease progression and subsequently died. However, given the increasing availability of targeted treatments, NGS plays a critical role in identifying actionable genetic alterations. Cytological samples (including smears, and cell blocks), as well as small biopsy specimens, are generally suitable for NGS. Nevertheless, pre-analytical limitations—such as necrosis, low cellularity, or poor preservation—can affect various types of specimens, including smears, cell blocks, and small biopsies. These factors may compromise the quality of nucleic acid extraction and, consequently, the reliability of downstream molecular analyses. Reliable NGS requires a minimum tumour cell content of approximately 10–20% to avoid dilution by normal DNA. However, even small amounts of input DNA (<10 ng) from carefully selected tumour cells may be sufficient for analysis, highlighting the importance of accurate sample selection and preparation.

In addition, sample selection should also take into account the potential need to validate molecular profiling results using orthogonal methods. This may be required not only for diagnostic confirmation, as in the present case, but also for predictive purposes in the context of targeted therapy selection. This underscores the importance of rigorously assessing sample adequacy for both morphological and molecular analyses, acknowledging potential limitations, and, when necessary, pursuing additional or alternative tissue sampling. Such practices are essential to ensure diagnostic accuracy and, whenever possible, to guide therapeutic decision-making.

Conclusion

By anticipating diagnostic and predictive needs early in the diagnostic workflow, clinicians and pathologists can optimize specimen management, minimize the risk of inconclusive or inaccurate laboratory results, and ultimately improve patient care through more accurate diagnoses and better-informed therapeutic decisions.

Key points

- ATC can be difficult to diagnose due to low cellularity, necrosis, lack of typical thyroid markers, and overlapping features with other high-grade tumors, especially when supported by molecular findings.
- A fit-for-purpose approach to sample selection improves diagnostic accuracy and supports, when feasible, appropriate therapeutic decisions.

Literature

Podany P, Abi-Raad R, Barbieri A, Garritano J, Prasad ML, Cai G, et al. **Anaplastic thyroid carcinoma: Cytomorphologic features on fine-needle aspiration and associated diagnostic challenges.** Am J Clin Pathol [Internet]. 2022 Apr 1 [cited 2025 Sep 1];157(4):608–19. Available from: <http://dx.doi.org/10.1093/ajcp/aqab159>

Jin M, Jakowski J, Wakely PE Jr. **Undifferentiated (anaplastic) thyroid carcinoma and its mimics: a report of 59 cases.** J Am Soc Cytopathol [Internet]. 2016 Mar [cited 2025 Sep 1];5(2):107–15. Available from: <http://dx.doi.org/10.1016/j.jasc.2015.08.001>

Bible KC, Kebebew E, Brierley J, Brito JP, Cabanillas ME, Clark TJ Jr, et al. **2021 American Thyroid Association guidelines for management of patients with anaplastic thyroid cancer: American thyroid association anaplastic thyroid cancer guidelines task force.** Thyroid [Internet]. 2021 Mar [cited 2025 Sep 1];31(3):337–86. Available from: <http://dx.doi.org/10.1089/thy.2020.0944>

Bellevicine C, Malapelle U, Vigliar E, Pisapia P, Vita G, Troncone G. **How to prepare cytological samples for molecular testing.** J Clin Pathol [Internet]. 2017 Oct;70(10):819–26. Available from: <http://dx.doi.org/10.1136/jclinpath-2017-204561>

Cappello F, Angerilli V, Munari G, Ceccon C, Sabbadin M, Pagni F, et al. **FFPE-based NGS approaches into clinical practice: The limits of glory from a pathologist viewpoint.** J Pers Med [Internet]. 2022 May 5 [cited 2025 Sep 1];12(5):750. Available from: <http://dx.doi.org/10.3390/jpm12050750>

Tsao MS, Yatabe Y. **Old soldiers never die: Is there still a role for immunohistochemistry in the era of next-generation sequencing panel testing?** J Thorac Oncol [Internet]. 2019 Dec;14(12):2035–8. Available from: <http://dx.doi.org/10.1016/j.jtho.2019.09.007>

Song J, Gersten A, Herzberg B, Halmos B. **Thoracic SMARCA4-deficient undifferentiated tumor: diagnostic characteristics, molecular insights, and treatment approaches.** Oncologist [Internet]. 2025 May 8 [cited 2025 Sep 1];30(5):oyaf121. Available from: <https://dx.doi.org/10.1093/oncolo/oyaf121>